CORRECTION AND SCOPE

Bounded Clock Realization of an Axis-Reduced Auxiliary Tensor Code: Positive Many-Body Spectra and a Three-Dimensional Locality Obstruction

Correction to the radius-two local-generator count on manuscript page 7. The small periodic box gave 12 Z and 14 X operators. The wrap-free calculation gives five Z and five X generators. The axis-reduced construction and its stated finite-box spectra retain their separate scope.

Manuscript · p. 7, radius-two table

Three-Dimensional Local Logical Pairing and a Finite-Range Compact No-Go

Evidence · Corrected three-dimensional local logical pairing

Bounded Clock Realization of an Axis-Reduced Auxiliary Tensor Code

Positive many-body spectra and a three-dimensional locality obstruction

Joshua Farrow
Independent Research

June 2026

Abstract

We test whether the previously derived auxiliary-register tensor parent can be realized by a bounded local Villain or clock Hamiltonian whose actual many-body spectrum contains two linearly dispersing transverse-traceless (TT) modes while constraint defects remain gapped. A positive construction is obtained for the exact one-dimensional reduction associated with propagation along a fixed lattice axis. The finite-field code uses six symmetric-tensor and six auxiliary clock registers per site, has exactly commuting gauge and scalar stabilizers, and contains two local canonical TT clock pairs per site. Exact diagonalization of finite open-shift quantum-link rotors and cyclic $\mathbb{Z}_p$ clocks produces finite-size spectra consistent with two degenerate $z = 1$ branches over finite coupling windows. A logical-symmetry-breaking control opens a nonzero mass, while symmetry-preserving local perturbations retain the soft branch over the tested sizes. The constraint defect gap is finite at every fixed clock dimension; retaining a nonzero gap as $p \to \infty$ requires the usual Villain scaling of the stabilizer coefficient, $\Delta_p \propto p^2$. The generic three-dimensional result is negative: on an $L = 5$ torus the complete local commutant has no nontrivial onsite or radius-one physical logical operators, and nontrivial logicals first appear at radius two. Thus the bounded axis-reduced realization is established, but a generic three-dimensional compact $z = 1$ TT phase is not.

1 Question and status

The preceding quadratic auxiliary construction generated the lattice Einstein kernel as an exact Schur complement and gave two $z = 1$ TT branches after imposing the scalar constraint. Its unresolved step was microscopic: could the construction be implemented using bounded local register operators, with a finite defect gap and the same two branches in the spectrum of an actual many-body Hamiltonian?

The answer obtained here is deliberately split into two statements:

1. For a wave vector constrained to a fixed lattice axis, the answer is yes. The modular code admits two local TT clock pairs and a bounded local logical Hamiltonian.
2. For generic three-dimensional propagation, the same onsite factorization fails. The first nontrivial local physical operators found by the commutant audit have Manhattan radius two.

The second point prevents the directional construction from being advertised as a complete three-dimensional helicity-2 phase.

2 Axis-reduced modular tensor code

2.1 Clock algebra and registers

Let p be an odd prime, $\omega = e^{2\pi i/p}$, and let each qudit carry clock operators

$$ZX = \omega XZ, \qquad X^p = Z^p = I. \tag{1}$$

At every site we introduce six tensor clocks

$$h = (h_{xx}, h_{yy}, h_{zz}, h_{xy}, h_{xz}, h_{yz}) \tag{2}$$

and six auxiliary clocks y_a. For propagation along the x axis, a periodic central difference D acts only along the chain. The extended gauge action is written as

$$\delta h = D_h \xi, \qquad \delta y = -\frac{1}{2} L D_h \xi, \tag{3}$$

where D_h is the axis-reduced symmetric-gradient map and L is the first-order operator inherited from the auxiliary parent. The invariant auxiliary stabilizers are

$$u = y + \frac{1}{2}Lh, \tag{4}$$

and the exact scalar stabilizer is

$$C_0 = -D^2(h_{yy} + h_{zz}). \tag{5}$$

All arithmetic in the stabilizer audit is performed exactly over GF(p).

2.2 Local TT logical clocks

For this directional reduction the two TT polarizations become local:

$$Z_{+,x} = Z^{(h_{yy,x} - h_{zz,x})/2}, \qquad X_{+,x} : (h_{yy,x}, h_{zz,x}) \mapsto (h_{yy,x} + 1, h_{zz,x} - 1), \tag{6}$$

$$Z_{\times,x} = Z^{h_{yz,x}}, \qquad X_{\times,x} : h_{yz,x} \mapsto h_{yz,x} + 1. \tag{7}$$

They commute with every gauge, auxiliary, and scalar stabilizer, and obey two independent canonical clock algebras. In particular,

$$Z_{\lambda,x} X_{\lambda',x'} = \omega^{\delta_{\lambda\lambda'}\delta_{xx'}} X_{\lambda',x'} Z_{\lambda,x}, \qquad \lambda \in \{+, \times\}. \tag{8}$$

For $p = 13$ and odd $L = 3, 5, 7, 9, 11$, every commutator and canonical-pair residual is exactly zero. The ranks are

$$\operatorname{rank} X = 3(L-1), \qquad \operatorname{rank} Z = 7L - 1, \tag{9}$$

so the number of logical qudits is

$$12L - 3(L-1) - (7L-1) = 2L + 4. \tag{10}$$

The $2L$ extensive logicals are the two local TT clocks; four are global zero modes.

Table 1: Exact finite-field stabilizer audit at $p = 13$.

L	registers	rank X	rank Z	logical	$2L+4$
3	36	6	20	10	10
5	60	12	34	14	14
7	84	18	48	18	18
9	108	24	62	22	22
11	132	30	76	26	26

A regulator caveat is visible when p divides L: for the tested pairs $p = L = 5, 7, 11, 13$, the discrete derivative acquires an extra finite-field kernel and one additional logical qudit appears. The primary audits therefore use $p \nmid L$.

3 Bounded local Hamiltonian and defect gap

A bounded code Hamiltonian can be written as

$$H_{\text{code}} = -\Delta_G \sum \operatorname{Re} A - \Delta_u \sum \operatorname{Re} U - \Delta_0 \sum \operatorname{Re} B + H_+ + H_\times, \tag{11}$$

where A, U, B denote the commuting gauge, auxiliary, and scalar stabilizers. Each polarization is assigned a local clock Hamiltonian

$$H_\lambda = -\frac{J}{2} \sum_x \left(Z_{\lambda,x} Z^\dagger_{\lambda,x+1} + \text{h.c.} \right) - \frac{g}{2} \sum_x \left(X_{\lambda,x} + \text{h.c.} \right). \tag{12}$$

Because all logical operators commute with the stabilizers, the spectrum decomposes exactly into logical dynamics plus syndrome energies. No infinite penalty is needed at fixed p.

For a stabilizer term $-\Delta \operatorname{Re} S$, the smallest nontrivial syndrome costs

$$\Delta_{\text{def}}(p) = \Delta \left[1 - \cos\left(\frac{2\pi}{p} \right) \right]. \tag{13}$$

At fixed Δ, this vanishes as p^{-2}. A clock-to-rotor limit with a uniform defect gap requires

$$\Delta_p = \frac{p^2}{2\pi^2}\Delta_*, \tag{14}$$

for which $\Delta_{\mathrm{def}} \to \Delta_*$. This scaling is a substantive qualification: the finite-p Hamiltonian is bounded, but a fixed-coefficient $p \to \infty$ sequence does not retain the defect gap.

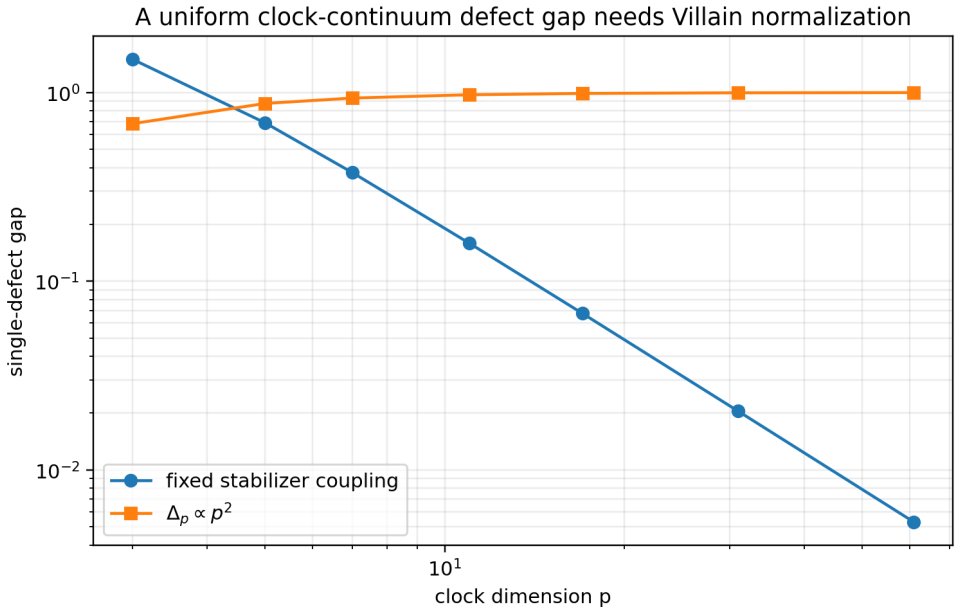

Figure 1: Single-defect gap versus clock dimension. Fixed stabilizer coefficients give a p^{-2} closing gap; Villain normalization keeps the gap finite.

4 Bounded quantum-link rotor spectrum

To test the logical dynamics independently of cyclic wraparound, we first use a finite open-shift rotor with local basis $n = -S, \ldots, S$ and $d = 2S + 1$:

$$H_{\mathrm{rot}} = \frac{U}{2}\sum_x n_x^2 - \frac{J}{2}\sum_x \left(R_x R_{x+1}^\dagger + \mathrm{h.c.}\right) + V\sum_x n_x n_{x+1} - \frac{J_2}{2}\sum_x \left(R_x R_{x+2}^\dagger + \mathrm{h.c.}\right). \tag{15}$$

The shift R annihilates the top state rather than wrapping around. Total charge $Q = \sum_x n_x$ is exact. We block diagonalize by Q and momentum, and extract the lowest pole with nonzero density spectral weight at $k_{\mathrm{min}} = 2\pi/L$.

The dispersion diagnostic is

$$\omega^2(k) = m_{\mathrm{fit}}^2 + v_{\mathrm{fit}}^2 \widehat{k}^2, \qquad \widehat{k} = 2\sin(k/2). \tag{16}$$

Small negative fitted intercepts are interpreted only as finite-size consistency with zero, not as physical tachyonic masses.

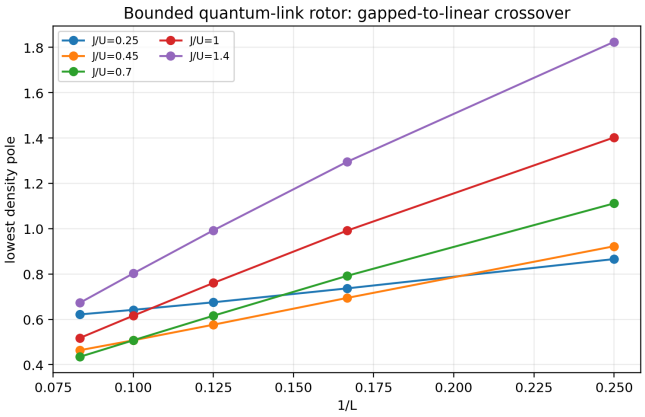

(a) Finite-size scan at $d = 3$.

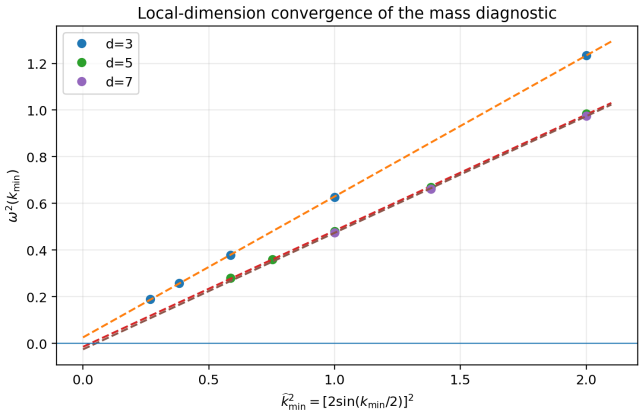

(b) Mass diagnostic at $J/U = 0.7$.

Figure 2: Bounded rotor spectra. The low-coupling control remains massive, whereas intermediate couplings develop a stable $\omega/\hat{k}$ ratio.

Table 2: Selected mass fits. Two identical logical copies give two degenerate TT branches.

d	J/U	sizes	m^2_{fit}	v_{fit}	status
3	0.25	5	0.331800	0.457358	gapped control
3	1.00	5	0.003927	0.990250	near-massless
5	0.45	5	0.063620	0.579269	gapped control
5	0.70	5	-0.014806	0.705479	zero-consistent
5	1.00	5	-0.022154	0.852748	zero-consistent
7	0.70	3	-0.025777	0.706812	cutoff check
7	1.00	3	-0.036977	0.846831	cutoff check

The ratio $\omega/\hat{k}$ is particularly transparent. At $d = 5$, $J/U = 0.7$, it changes from 0.7012 at $L = 4$ to approximately 0.691 at $L = 8$; at $J/U = 1$ it changes from 0.8472 to 0.8339. This is the strongest finite-size evidence for a linear branch in the directional model.

Symmetry-preserving density and next-neighbor perturbations leave a soft pole across $L = 6, 8, 10, 12$, although four sizes are insufficient to establish an infinite-volume phase boundary.

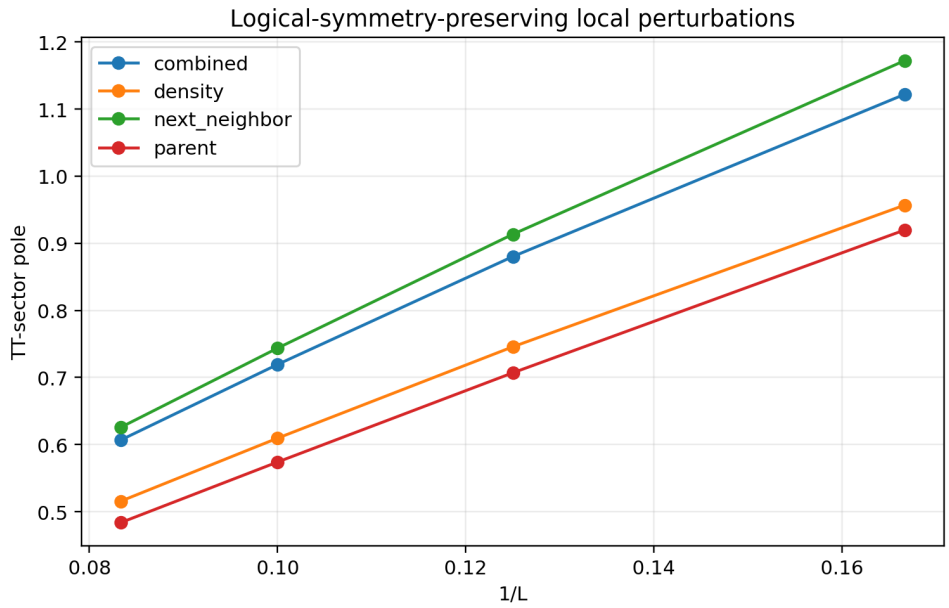

Figure 3: The directional soft branch under several local perturbations that preserve total logical charge.

5 Exact cyclic-clock regulator

The open-shift truncation is complemented by a genuinely cyclic $\mathbb{Z}_p$ chain,

$$H_p = -\frac{J}{2}\sum_x \left(Z_x Z_{x+1}^\dagger + \text{h.c.}\right) - \frac{g}{2}\sum_x \left(X_x + \text{h.c.}\right). \tag{17}$$

The Hamiltonian is diagonalized exactly in total $\mathbb{Z}_p$ charge and momentum sectors. For $p = 5$ and $L = 4, \ldots, 8$, the mass diagnostic separates the controls $J/g = 0.6$ and 1.67 from a finite-size zero-mass window near $0.8 \leq J/g \leq 1.25$.

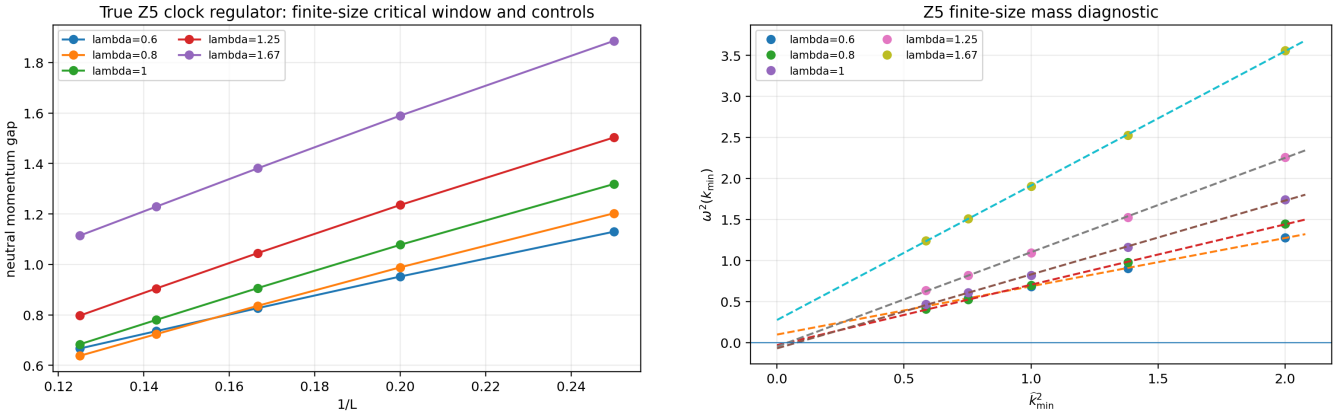

(a) Neutral momentum gaps.

(b) Relativistic mass diagnostic.

Figure 4: Finite-size $\mathbb{Z}_5$ clock spectra. The data support a critical window but are not used to claim precise transition locations.

Table 3: $\mathbb{Z}_5$ mass fits from $L = 4$–8.

J/g	$m^2_{\rm fit}$	$v_{\rm fit}$	R^2	interpretation
0.60	0.097347	0.766873	0.999925	gapped control
0.80	-0.031303	0.857718	0.999728	zero-consistent
1.00	-0.070821	0.948879	0.999613	zero-consistent
1.25	-0.048911	1.072147	0.999728	zero-consistent
1.67	0.274936	1.279699	0.999926	gapped control

The $p = 7$ data at $L = 4$–7 show approximately $1/L$ gaps over all tested couplings, but those sizes do not locate the phase boundaries. No precise critical coupling is inferred.

6 Mass-generation control

The reduced model possesses an exact total logical-charge symmetry. To verify that the soft mode is not a generic finite-size artifact, we add an onsite open-shift perturbation

$$H_{\rm break} = -\frac{h}{2}\sum_x (R_x + R_x^\dagger), \tag{18}$$

which changes total charge. Exact diagonalization in the full product Hilbert space gives a lowest-gap extrapolation of approximately 0.274, 0.425, and 0.606 for $h = 0.08$, 0.16, and 0.30, respectively. The unbroken scan is consistent with a vanishing gap over the available sizes.

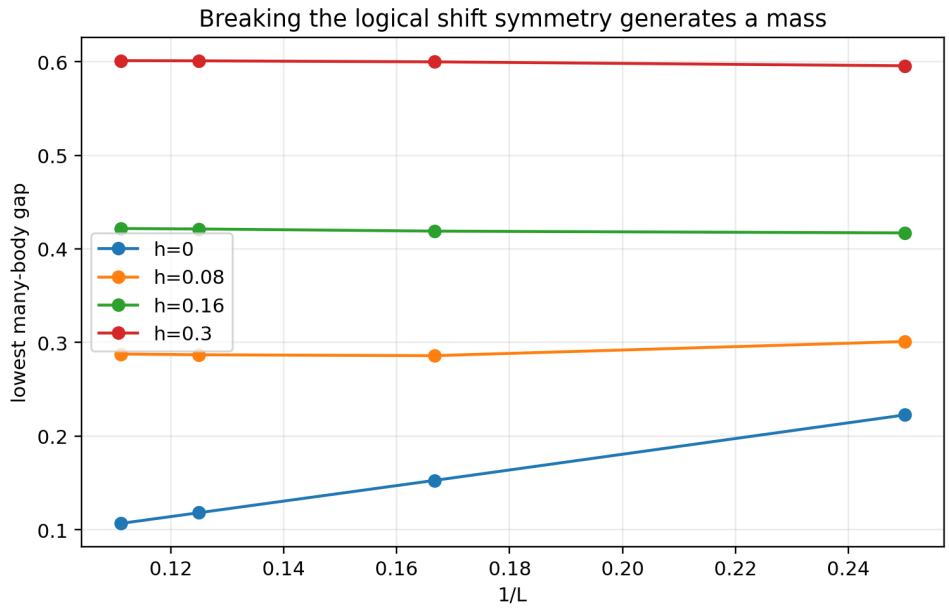

Figure 5: A logical-symmetry-breaking onsite shift opens a clear mass in the directional model.

7 Bounded auxiliary mode

A finite open-shift auxiliary oscillator with onsite Hamiltonian

$$H_y = 0.85\, n_y^2 - 0.55(R_y + R_y^\dagger) \tag{19}$$

has a rapidly convergent gap: 1.31135 at $d = 3$, 1.21874 at $d = 5$, and 1.217123342 by $d = 11$. Thus a bounded auxiliary register can remain gapped while the logical TT sector is soft. This is a local spectral check, not a proof that the complete three-dimensional phase exists.

8 Three-dimensional local-commutant audit

The decisive limitation appears when the complete six-component plus six-auxiliary CSS construction is placed on an $L = 5$ cubic torus. There are $12L^3 = 1500$ qudits. Exact sparse rank calculations over GF(7) give

$$\operatorname{rank} X = 372, \qquad \operatorname{rank} Z = 874, \tag{20}$$

leaving

$$1500 - 372 - 874 = 254 = 2L^3 + 4 \tag{21}$$

logical qudits, as expected globally.

The local question is different. For a Manhattan ball of radius R, we calculate the dimension of physical X and Z operators supported entirely in the ball, modulo stabilizers of the same support. The result is

R	sites	Z logical dimension	X logical dimension
0	1	0	0
1	7	0	0
2	25	12	14

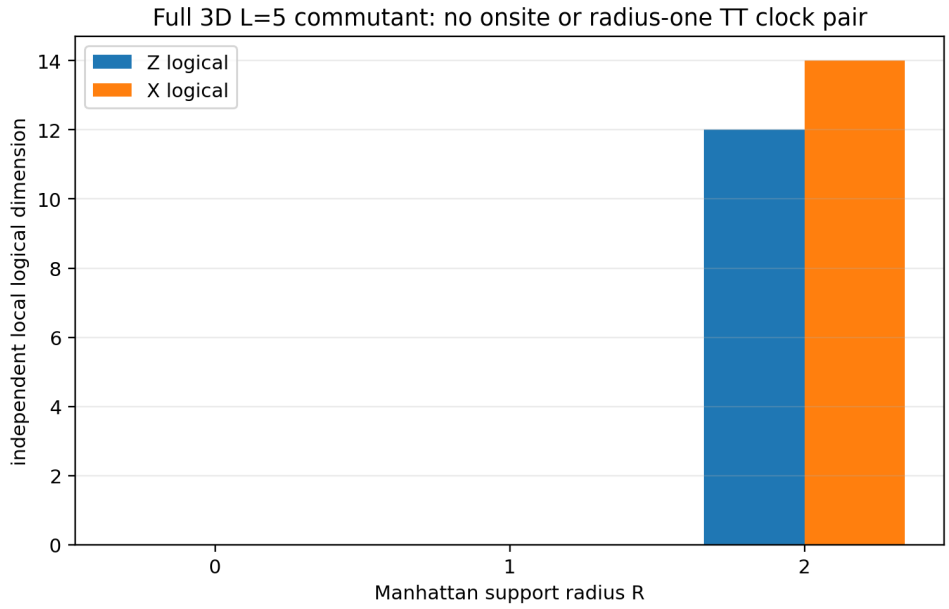

Figure 6: The full three-dimensional code has no nontrivial onsite or radius-one physical logical operator in the $L = 5$ audit.

The absence at $R = 0, 1$ means that the local plus/cross clock factorization used in the axis reduction does not extend directly to generic momentum. Radius-two physical operators exist, but this calculation has not yet shown that they form translation-covariant canonical pairs or that a bounded local Hamiltonian built from them has a positive k^2 TT kernel. Therefore this audit is an obstruction to the naive extension, not a no-go theorem for every auxiliary construction.

9 Verdict and next calculation

The correct conclusion is

> A bounded local finite-register realization exists for the exact propagation-axis reduction of the modular auxiliary tensor code. It has two exact local TT logical clocks, a finite stabilizer defect gap at every fixed clock dimension, and many-body spectra consistent with two linearly dispersing branches over finite coupling windows. A uniform defect gap in the $p \to \infty$ sequence requires Villain scaling. The generic three-dimensional bounded local $z = 1$ realization remains unestablished.

The next decisive calculation is no longer another one-dimensional size scan. It is to extract the radius-two three-dimensional logical bases, compute their symplectic pairing, and ask whether they can be assembled into translation-covariant local canonical variables. One must then enumerate all bounded-range quadratic Hamiltonians in that commutant. If every compact invariant begins at k^4, the observed obstruction should be promoted to a finite-range no-go theorem. If a positive k^2 TT kernel exists, that Hamiltonian should be diagonalized as the first genuine three-dimensional bounded regulator.

Reproducibility

The archive includes every raw exact-diagonalization point, the exact finite-field audits, the sparse $L = 5$ locality calculation, plotting scripts, aggregate JSON, and checksums. The main numerical environment was Python 3.13.5, NumPy 2.3.5, SciPy 1.17.0, and Matplotlib 3.10.8.